



Halocarbons as Hydrogen Bond Acceptors: A Spectroscopic Study of Haloethylbenzenes (PhCH₂CH₂X, X=F, Cl, Br) and their Hydrate Clusters

Journal:	<i>Physical Chemistry Chemical Physics</i>
Manuscript ID	CP-ART-10-2017-007365.R1
Article Type:	Paper
Date Submitted by the Author:	15-Feb-2018
Complete List of Authors:	Robertson, Patrick; Latrobe University, Chemistry & Physics Villani, Luigi; Latrobe University, Chemistry & Physics Dissanayake, Uresha; Latrobe University, Chemistry & Physics Duncan, Luke; La Trobe University, Chemistry and Physics Abbott, Belinda; La Trobe University, Chemistry Wilson, David; La Trobe University, Chemistry Robertson, Evan; Latrobe University, chemistry

Halocarbons as Hydrogen Bond Acceptors: A Spectroscopic Study of Haloethylbenzenes (PhCH₂CH₂X, X=F, Cl, Br) and their Hydrate Clusters

Patrick A. Robertson, Luigi Villani, Uresha L. M. Dissanayake, Luke F. Duncan, Belinda M. Abbott, David J. D. Wilson, Evan G. Robertson*

Department of Chemistry and Physics, La Trobe Institute for Molecular Science, La Trobe University, Melbourne, 3086, Australia.

* correspondence should be directed to e.robertson@latrobe.edu.au

Abstract

The electronic spectrum of 2-bromoethylbenzene and its chloro and fluoro analogues have been recorded by resonant two-photon ionisation (R2PI) spectroscopy. *Anti* and *gauche* conformers have been assigned by rotational band contour analysis and IR-UV ion depletion spectroscopy in the CH region. Hydrate clusters of the *anti* conformers have also been observed, allowing the role of halocarbons as hydrogen bond acceptors to be examined in this context. The donor OH stretch of water bound to chlorine is red-shifted by 36 cm⁻¹, or 39 cm⁻¹ in the case of bromine. Although classed as weak H-bond acceptors, halocarbons are favourable acceptor sites compared to π systems. Fluorine stands out as the weakest H-bond acceptor amongst the halogens. Chlorine and bromine are also weak H-bond acceptors, but allow for more geometric lability, facilitating complimentary secondary interactions within the host molecule. *Ab initio* and DFT quantum chemical calculations, both harmonic and anharmonic, aid the structural assignments and analysis.

Introduction

The hydrogen-bond accepting capability of halogens has been the subject of interest for the past two decades.¹⁻⁴ Hydrogen bonding to halide ions has been studied extensively, due to the abundance of halide ions in various biologically important ion channels (chloride ions), as well as the role of halide salts in waste remediation.^{5,6} In the realm of atmospheric chemistry, free halogen atoms react in a variety of processes in the stratosphere and troposphere, ultimately forming organic halogen compounds.⁷ Synthetic organometallic chemistry frequently exploits metal-halides, specifically as Grignard reagents (R-M-X).⁸ Of particular interest is the role of halocarbon systems in supramolecular self-assembly; weak hydrogen bonds are extremely helpful in guiding and complimenting stronger forces, and organic halides offer the potential for chemically tuneable directionality. Recently, there has been increased interest in the use of halogenated compounds as templates for supramolecular assemblies and self-assembly.^{9,10} Finally, the widespread use of halogenated organic compounds as solvents in organic synthesis and crystallisation should highlight the importance of improving our understanding of these compounds, and the relevance of their hydrogen bond acceptor capabilities.

The hydrogen-bond acceptor capabilities of halogen atoms vary widely with the intrinsic chemistry of the halogen itself, as well with that of its local chemical environment. Halide species such as FHF^- are well-known to be amongst the strongest H-bond acceptors observed to date; it and other anionic halide cluster systems have been explored extensively.^{11,12} The behaviour of organic halides (X-C) as H-bond acceptors with water has been comparatively less widely studied. Organic halides are generally considered weak hydrogen bond acceptors; there are comparatively few examples of O-H...X-C complexes in the Cambridge Crystallographic Database, compared either anionic or metal-halide systems.¹⁰

Nonetheless, weak attractive forces are critical for determining conformation and intermolecular interactions, and these “non-conventional” hydrogen bonds are almost ubiquitous in biological systems.

The present study builds upon previous work within our research group,¹³ with the aim of highlighting the hydrogen bond acceptor properties of halocarbons by investigating three halogen species in a flexible organic framework. The electronic and vibrational spectra of three haloethylbenzene molecules (PhCH₂CH₂X, X = F, Cl, Br) are studied by resonance enhanced multi-photon ionisation spectroscopy, coupled to time-of-flight mass spectrometry. Hydrated analogues of each molecule (XEB.w₁), spectroscopically observed in the molecular beam and analysed with the aid of *ab initio* and DFT calculations, provide a window into the strengths and geometric tendencies of hydrogen bonds with halocarbon acceptors.

Experimental

Spectroscopy

The R2PI-TOF setup used has been described in elsewhere^{14,15}, the specifics relating to this study are as follows. 2-Bromoethylbenzene (BrEB) and 2-chloroethylbenzene (CEB) were purchased from Sigma-Aldrich and used as received. 2-Fluoroethylbenzene (FEB) was synthesised as per the procedure detailed by Lal *et al.*¹⁶ Free jet expansion conditions of the haloethylbenzene compounds required heating the liquid samples to 373 K, 363 K and 343 K for BrEB, FEB, and CEB, respectively. Argon carrier gas was passed over the heated samples (pressure 1.5 bar), and the argon-XEB mixture was pulsed (10 Hz) into a vacuum through an orifice (diameter 0.8 mm). The coldest part of the resulting expansion was picked off by a skimmer (1.5 mm, 20 mm downstream from the orifice) and the resulting molecular beam was intersected at right-angles by the

frequency-doubled output of a tuneable dye laser (Coumarin 540). In all experiments, one colour resonant two-photon ionisation (1C-R2PI) was sufficient to cause ionisation.

Conformer specific IR-UV spectra were recorded by intersecting the molecular beam with the output of a tuneable IR OPO/OPA (laser vision), anti-parallel relative to the UV source, timed to arrive ~400 ns prior to the ionisation laser pulse.

Theoretical

All quantum chemical calculations were performed using the Gaussian 09 software package.¹⁷ The geometries of all monomers and single water clusters were optimised using both B3LYP with Grimme's empirical dispersion correction together with Becke-Johnson damping,¹⁸ B3LYP-D3(BJ), and MP2 levels of theory. Basis sets employed were 6-311++G(d,p), aug-cc-pVTZ, and def2-TZVPP. Harmonic frequency calculations were carried out only for B3LYP-D3(BJ) optimized geometries. Single-point energies were calculated for the MP2 optimised geometries at the CCSD(T)-F12/cc-pVDZ-F12 level of theory for FEB and CEB, and CCSD(T)-F12/cc-pVDZ for BrEB. Aliphatic CH stretch modes of each monomer were also predicted by a simplified anharmonic method developed by Tabor *et al*¹⁹⁻²² using B3LYP, B3LYP-D3 and ω B97X-D levels of theory with the 6-311++G(d,p) basis set. Excited state properties of BrEB were investigated using configuration-interaction singles (CIS) theory with a 6-31G(d) basis set since that level of theory has been extensively used and benchmarked for $S_1 \leftarrow S_0$ transition dipole moment (TDM) calculations on similar molecules.²³ Simulated rotational contours were generated using S_0 and S_1 rotational constants from HF/6-31G(d) and CIS/6-31G(d) calculations, and hybrid band compositions from the TDM's at the CIS/6-

31G(d)//HF/6-31G(d) level. Remaining simulation parameters such as rotational temperature, and resolution were optimised empirically.

Results

Theoretical

Anti and *gauche* conformers have been identified for the BrEB monomer and are shown in Figure 1. These structures are analogous to those reported previously for CEB and FEB.¹³ Relative energies and binding energies for all monomer and XEB-water clusters are presented in Table 1. The *anti* conformer of all three halocarbon monomers was found to be the most stable with all levels of theory and basis set, with the exception of the *gauche* monomer of BrEB at MP2/aug-cc-pVTZ, consistent with previous studies of propylbenzene²⁴ and benzenepropanenitrile.^{14,25}

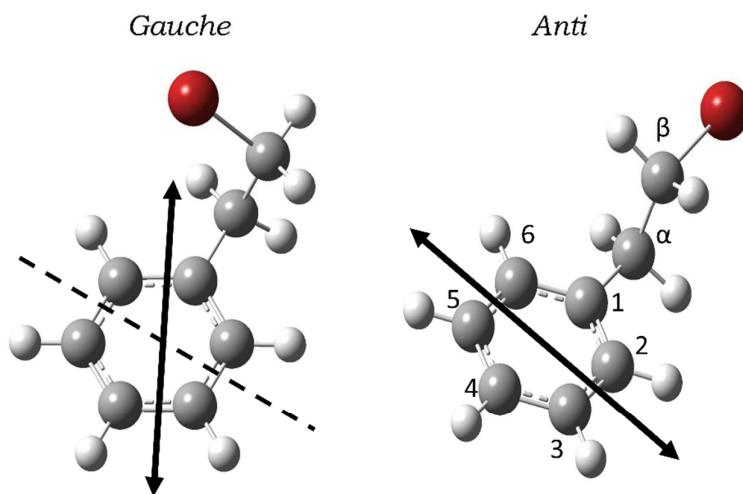


Figure 1. *Gauche* and *anti* conformers of BrEB calculated at MP2/aug-cc-pVTZ level. Predicted S_1 - S_0 transition dipole moment alignments at CIS/6-31G(d) level are also shown, corresponding to $\theta_{elec}=69^\circ$ (*gauche*) and 0° (*anti*).

Table 1. Relative energies (kJ mol^{-1}) of XEB monomers in the equilibrium state (U_e) and zero-point corrected state (U_0).

			FEB		CEB		BrEB	
			<i>Anti</i>	<i>Gauche</i>	<i>Anti</i>	<i>Gauche</i>	<i>Anti</i>	<i>Gauche</i>
B3LYP-D3	6-311++G**	U_e	0.0	2.0	0.0	2.1	0.0	2.2
		U_0	0.0	1.9	0.0	1.9	0.0	1.9
B3LYP-D3	aug-cc-pVTZ	U_e	0.0	2.0	0.0	2.1	0.0	1.9
		U_0	0.0	1.9	0.0	2.0	0.0	1.7
MP2	def2-TZVPP	U_e	0.0	1.6	0.0	1.4	0.0	0.9
		U_0	0.0	1.6	0.0	1.2	0.0	0.8
MP2	aug-cc-pVTZ ^a	U_e	0.0	1.8	0.0	1.0	0.4	0.0
		U_0	0.0	1.7	0.0	0.9	0.5	0.0
CCSD(T)-F12	cc-pVDZ-F12 ^{a,b}	U_e	0.0	1.8	0.0	2.4	0.0	2.6
		U_0	0.0	1.7	0.0	2.2	0.0	2.5

a) zero-point correction taken from MP2/aug-cc-pVTZ level.

b) cc-pVDZ-F12 basis set used for FEB and CEB. The cc-pVDZ basis set was employed in BrEB since the cc-pVDZ-F12 basis set is not available for Br.

Two singly-hydrated water clusters were identified for the host *anti* conformers of all FEB, CEB and BrEB species. The conformers are designated side-type and pi-type, based on the binding of water perpendicular to the halogen atom or to the aromatic ring, respectively. Two *gauche* hydrate structures were found, designated *gauche-pi* or *gauche-side* in an analogous fashion, but investigated less comprehensively because experimental IR spectra could be measured only for *anti* hydrate clusters. All XEB.w1 structures are reported in Figure 2, and relative energies are summarised in Table 2.

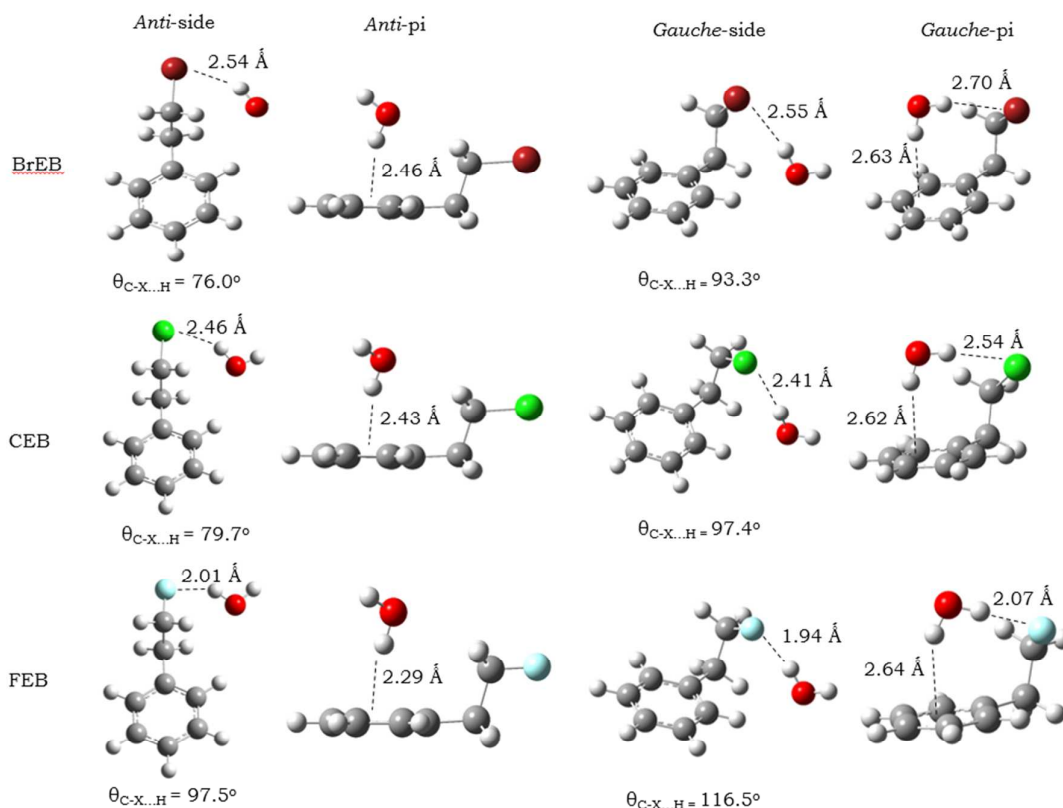


Figure 2. Predicted structures and geometric parameters for XEB.w₁ clusters. *Anti*-clusters are calculated at MP2/aug-cc-pVTZ level, *gauche* clusters at B3LYP-D3(BJ)/aug-cc-pVTZ.

Anti XEB-water clusters show a small (but consistent) preference for side-type structures over pi-type for all species and all levels of theory, with the exception of FEB with MP2/def2-TZVPP, and only after applying the zero-point correction. At the highest CCSD(T)-F12/cc-pVDZ-F12 level, and the cost-effective B3LYP-D3(BJ)/aug-cc-pVTZ level, the binding energies of the pi-type clusters are 12-14 kJ mol⁻¹, in line with the reported experimental binding energy of 12 kJ mol⁻¹ for the water benzene dimer.²⁶ At all levels of theory, an increase in H...XC bond distance is observed as we move down the periodic table (F<Cl<Br), and this trend is also observed in *gauche* clusters calculated at the B3LYP-D3(BJ)/aug-cc-pVTZ level of theory. The bond angle θ_{HXC} decreases with increased atomic radius (Br<Cl<F), illustrated in Figure 2. This finding is in accordance with geometries reported

previously in a study of anisotropic charge distribution in metal-halide and halocarbon systems.^{10,27}

Table 2. Relative energies and zero-point corrected binding energies (B.E.) of XEB. w_1 clusters (in kJ mol⁻¹).

			FEB		CEB		BrEB	
			pi	side	pi	side	pi	side
B3LYP-D3	6-311++G**	U_e	3.3	0.0	2.8	0.0	3.2	0.0
		U_0	0.7	0.0	1.5	0.0	2.2	0.0
		B.E.	16.7	17.3	16.6	18.1	16.6	18.7
B3LYP-D3	aug-cc-pVTZ	U_e	3.1	0.0	3.0	0.0	3.5	0.0
		U_0	0.9	0.0	2.0	0.0	1.7	0.0
		B.E.	12.8	13.8	13.3	15.2	13.8	15.4
MP2	def2-TZVPP	U_e	1.5	0.0	1.5	0.0	1.9	0.0
		U_0	0.0	0.9	0.0	0.3	0.3	0.0
		B.E.	16.8	15.8	17.2	16.9	17.3	17.6
MP2	aug-cc-pVTZ ^a	U_e	2.5	0.0	1.4	0.0	2.8	0.0
		U_0	0.3	0.0	0.4	0.0	1.0	0.0
		B.E.	15.3	15.6	17.7	18.1	19.5	20.5
CCSD(T)-F12	cc-pVDZ-F12 ^{a,b}	U_e	4.7	0.0	3.7	0.0	(4.5)	(0)
		U_0	2.3	0.0	2.6	0.0	(2.8)	(0)
		B.E.	12.2	14.5	12.9	15.5	(20.6)	(23.4)
B3LYP-D3	aug-cc-pVTZ		<u>G-pi</u>	<u>G-side</u>	<u>G-pi</u>	<u>G-side</u>	<u>G-pi</u>	<u>G-side</u>
		U_e	0.0	2.3	0.0	4.0	0.0	3.8
		U_0	0.0	2.2	0.0	3.5	0.0	3.2
	B.E.	18.1	15.9	18.4	14.9	18.3	15.0	

a) zero-point correction taken from MP2/aug-cc-pVTZ level.

b) cc-pVDZ-F12 basis set used for FEB and CEB. The cc-pVDZ basis set was employed for BrEB since the cc-pVDZ-F12 basis set is not available for Br: parantheses indicate that the results are not directly comparable with those of CEB and FEB.

Electronic Spectra of XEB Monomers

The electronic spectra of 2-fluoroethylbenzene and 2-chloroethylbenzene were recorded previously by Martin *et al.*¹³ These spectra were reproduced successfully by 1C-R2PI spectroscopy and are displayed in Figure 3, along with the electronic spectra of the 2-bromoethylbenzene ⁷⁹Br isotopologue. Spectra of ⁸¹BrEB were also recorded, but no apparent spectral differences were observed. Features A and G in the CEB and FEB spectra were previously assigned to the *anti* and *gauche* conformer origins by rotational band contour analysis, and the BrEB origins are labelled according to the assignments detailed below.

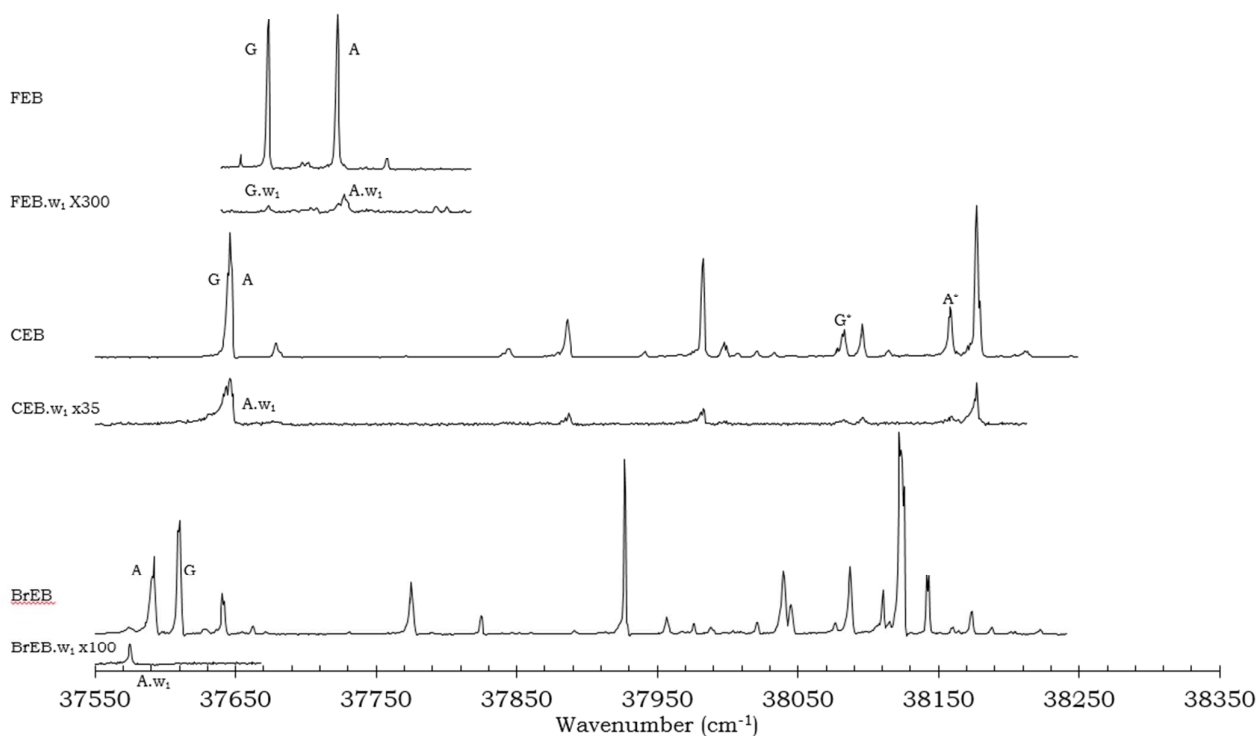


Figure 3. Normalised 1C-R2PI spectra of FEB, ³⁵CEB and ⁷⁹BrEB and respective one-water m/z channels, $(XEB.w_1)^+$.

Rotational band contour scans of BrEB origin bands A and G are shown in Figure 4, together with simulated band contours. The contour bands of CEB and FEB show similar band structures to those reported previously by Martin, *et al.*¹³ and support an assignment of band A to the *anti* conformer and band G to the *gauche* conformer. The A band of BrEB shows exclusively b-type character and the Q-subband spacing corresponds to a $2A-(B+C)$ value of ≈ 0.28 cm⁻¹ expected for the *anti* conformer. The *gauche* origin displays hybrid character consistent with rotation of the S₁-S₀ transition dipole moment in the molecular frame (Figure 1). The CIS/6-31G(d) prediction is $\theta_{\text{elec}}=69^\circ$, although a *gauche* simulation with less μ_a -type character corresponding to a smaller S₁-S₀ transition dipole moment rotation provides a slightly improved match to experiment. Previous studies have identified the sensitivity of the TDM of substituted benzenes to the conformation of the side chain.²³

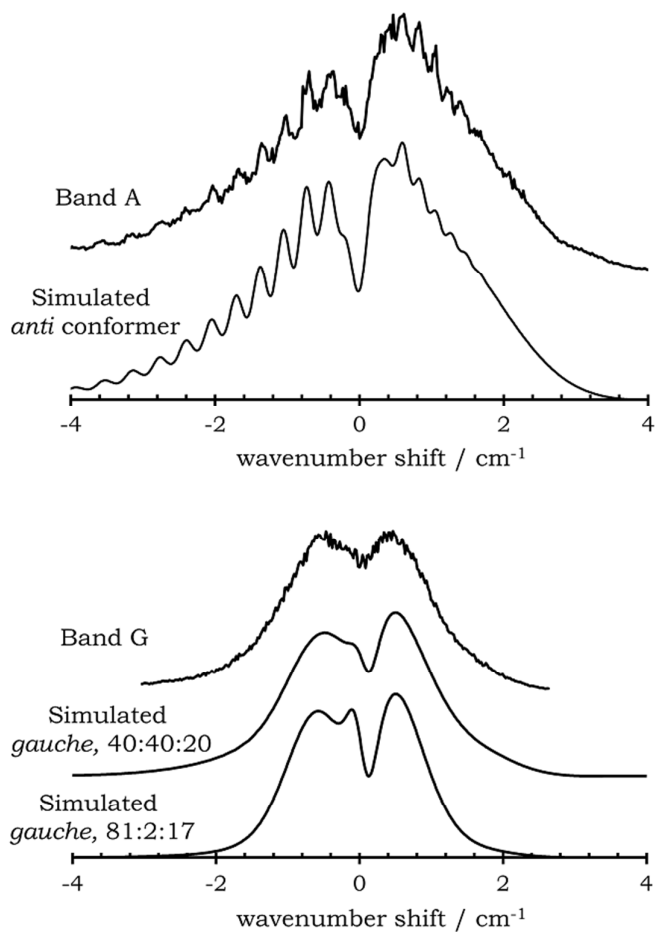


Figure 4. Rotational band contours of bands A and G of the BrEB electronic spectrum. Simulated band contours are also presented for comparison. Hybrid band parameters $\mu_a^2: \mu_b^2: \mu_c^2$ from CIS/6-31G(d) calculations are 0:100:0 ($\theta_{elec}=0^\circ$) for the anti and 81:2:17 ($\theta_{elec}=69^\circ$) for the gauche. $T_{rot} = 10$ K and linewidth = 0.20 cm^{-1} .

IR-UV ion depletion spectroscopy of XEB Monomers

Spectra of the CH stretch region between 2800 and 3150 cm^{-1} , recorded for features A and G of FEB and BrEB, and A* and G* of CEB, are shown in Figures 5, 6 and 7, respectively. Experimental band positions are summarised in Table 3.

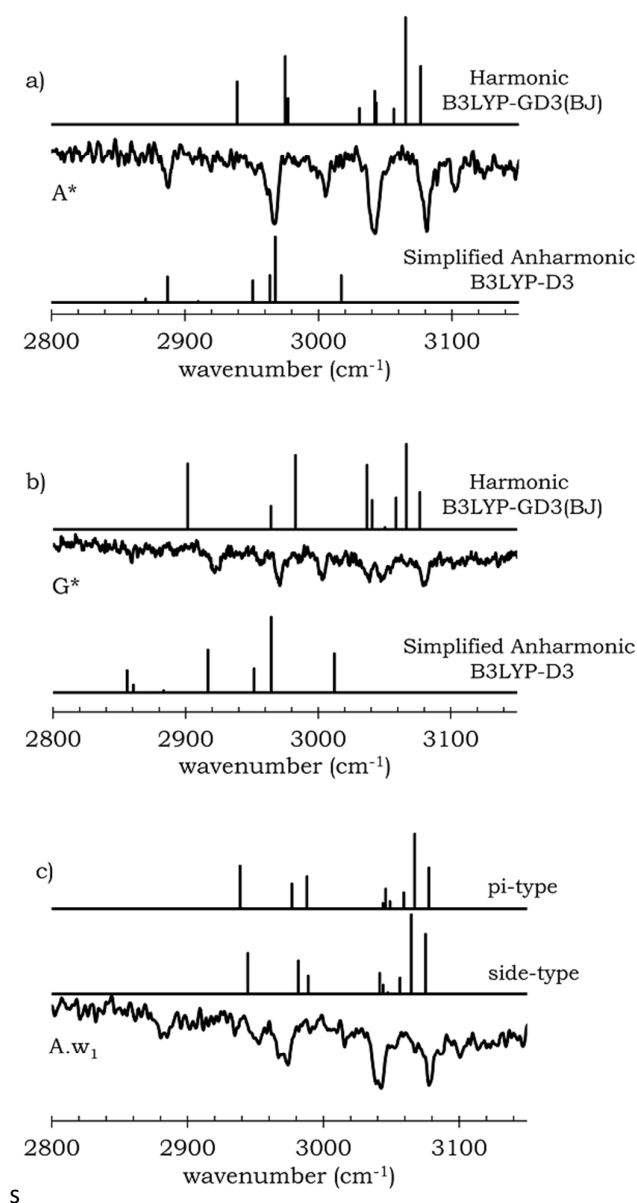


Figure 5. IR-UV ion-dip spectra of features a) A*, b) G* and c) A.w₁ of CEB/CEB.w₁ in the CH stretch region. Harmonic frequencies calculated at B3LYP-D3(BJ)/aug-cc-pVTZ (scaling factor = 0.967) are presented above the appropriate experimental traces. Anharmonic modelled aliphatic modes (B3LYP-D3/6-311++G(d,p)) are presented below experimental traces in a) and b).

In the aromatic CH stretch region the spectra of all three molecules show characteristic differences between the *anti* and *gauche* conformers. The same pattern is observed in benzenepropanenitrile¹⁴ and 2-phenylethanethiol,²⁸ thus providing a spectral signature enabling conformational assignment. Theoretical calculations provide insight into the reason for this. Stretch modes $\Gamma_{C2H-\Gamma_{C3H}} + \Gamma_{C6H-\Gamma_{C5H}}$, and $\Gamma_{C2H-\Gamma_{C3H}} - \Gamma_{C6H-\Gamma_{C5H}}$, corresponding to 13 and 7b respectively in Wilson's notation²⁹ are quasi-degenerate in energy in the *anti* conformer, but are partially decoupled due to the disruption of symmetry in the *gauche* conformer. This results in an observed red shift of mode 13-7b and a blue shift of mode 13+7b. Analysis of the B3LYP-D3(BJ)/aug-cc-pVTZ calculations indicate that these two normal modes are separated by less than a wavenumber in the *anti* conformer, and by up to 9 cm^{-1} in the *gauche* conformer of CEB. It is prudent to note that exact agreement between theoretical harmonic frequencies and experimental results for CH stretch region has been elusive, even at MP2 levels of theory.^{14,15} However, the spectral difference between *anti* and *gauche* conformers is consistent across all levels of theory, and although any absolute values at these levels of theory should be treated with healthy scepticism, the characteristic *anti-gauche* difference is a key indicator of monomer conformation for 2-substituted ethylbenzene derivatives.

Table 3. Experimental vibrational and electronic band positions (cm^{-1}) for all XEB and XEB. w_1 species.

BrEB			CEB			FEB	
A	G	A. w_1	A	G	A. w_1	A	G
2886	2861		2888	2893	2885	2891	
2953	2917		2959	2925	2953	2912	2908
2967	2961		2967	2957	2972	2960	2930
2986	2979			2971	1993		2952
3020	3020		3005	3003	3017	2980	2970
3043	3041		3043	3038	3043	3043	3038
	3049			3047	3053		3048
3084	3083		3082	3081	3078	3082	3079
3108	3106		3103	3102	3101	3104	3107
		3618			3621		
		3738			3737		
UV band positions			UV band positions			UV band positions	
A	37610		A	37646		A	37723
G	37591		G	37646		G	37673
A. w_1	37580		A*	38176		A. w_1	37729
			G*	38084		G. w_1	37676
			A. w_1	37646			

In the aliphatic CH stretch region, band positions and intensities differ between the A and G conformers. Application of the simplified anharmonic model of Tabor *et al.*²² considerably improves the agreement with experiment, compared with traditional harmonic frequency calculations. Figures 5-7 present the B3LYP-D3/6-311++G(d,p) simulations with the simplified anharmonic model, while the full results including those at B3LYP and ω B97X-D levels are included as supplementary data figures S1, S2 and S3. The anharmonic spectra incorporate seven states: four CH stretch fundamentals, two HCH scissor overtones and one HCH combination band. The model successfully captures the shifts in position and intensity that occur due to Fermi resonance induced mixing. Evident from the

anharmonic analysis are the very significant contribution from scissor overtone bands in the lower wavenumber region (*ca.* $<2900\text{ cm}^{-1}$) of the experimental spectrum, as found in both linear²² and cyclic alkylbenzenes¹⁹, and alkoxy species.²⁰

A noteworthy observation from the IR-UV spectra is that the highest wavenumber CH stretch mode, the antisymmetric $C_{\beta}H_2$ stretch, blue-shifts as the halogen atom increases in size ($F < Cl < Br$) for both *anti* and *gauche* conformers (40 cm^{-1} and 50 cm^{-1} , respectively). This observation is supported by all the harmonic and anharmonic frequency calculations (see table S1), with the shift slightly overestimated at DFT levels of theory, and underestimated with MP2. Experimental data on the highest energy (degenerate) CH stretch mode of CH_3X (3006 cm^{-1} , 3039 cm^{-1} and 3056 cm^{-1} for $X = F, Cl$ and Br , respectively) follows the same trend.³⁰ This ‘upshifting’ is also accompanied by a contraction of the $C_{\beta}-H$ bond ($Br < Cl < F$) and can potentially be attributed to interaction between the hydrogen atom and the increasingly diffuse and polarisable halogen atom, an interaction comparable to what Hobza has described as an “improper hydrogen bond”.³¹

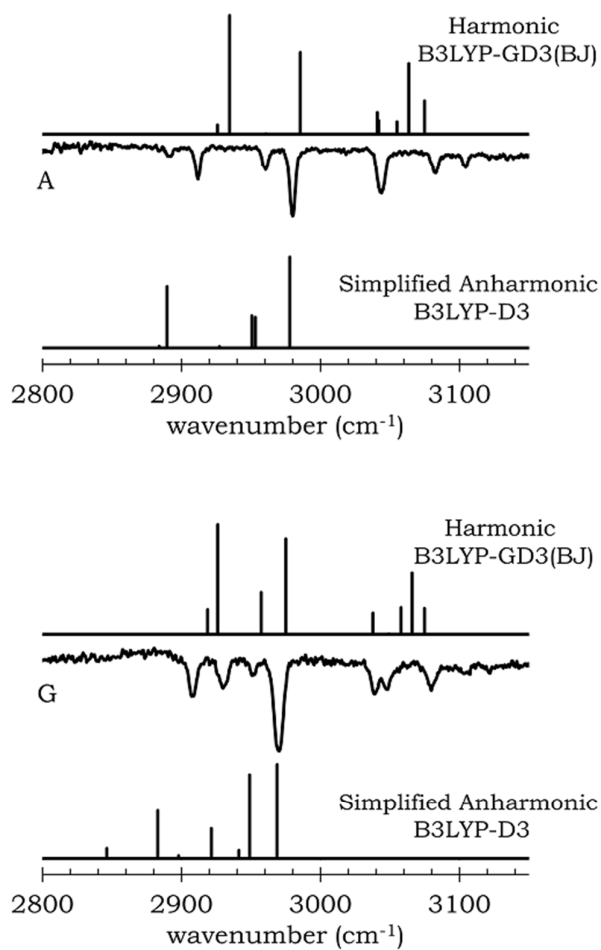


Figure 6. IR-UV ion-dip spectra in CH stretch region of features A and G of FEB. Harmonic frequency modes calculated at B3LYP-D3(BJ)/aug-cc-pVTZ (scaling factor = 0.967) are presented above, with anharmonic model (B3LYP-D3/6-311++G(d,p) aliphatic CH stretch, scissor overtone and combination bands presented below the experimental traces.

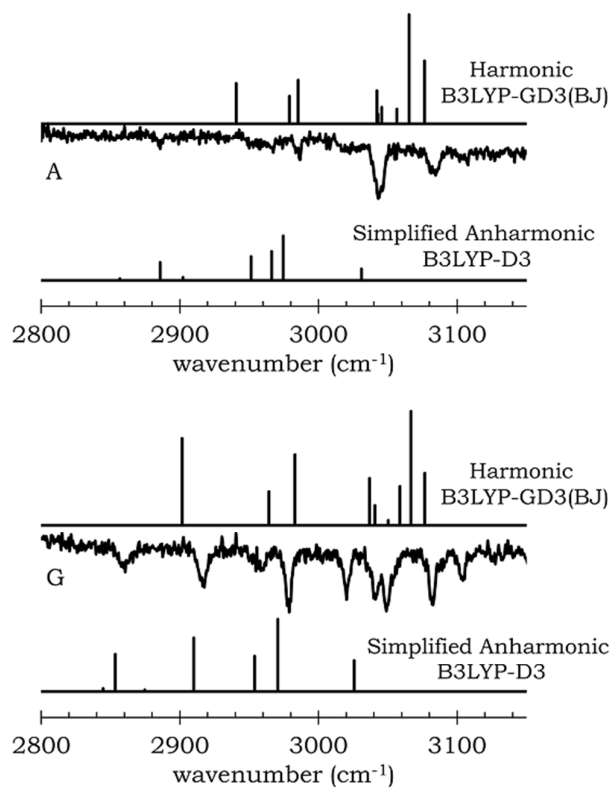


Figure 7. IR-UV ion-dip spectra in CH stretch region of feature A and G of BrEB. Harmonic frequency modes calculated at B3LYP-D3(BJ)/aug-cc-pVTZ (scaling factor = 0.967) are presented above, with anharmonic model (B3LYP-D3/6-311++G(d,p) incorporating aliphatic CH stretch, scissor overtone and combination bands) presented below the experimental traces.

Clusters

BrEB.w₁, CEB.w₁ and FEB.w₁ single water clusters were observed by monitoring the respective parent ion mass channel, and the resultant 1C-R2PI spectra are displayed in Figure 3.

The R2PI spectra of FEB.w₁ and CEB.w₁ accord with those reported previously by Martin *et al.*,¹³ and the close resemblance of the most significant vibronic features to those of the corresponding *anti* conformer (revealed by holeburning) was noted in that study. The inferred solvent-induced S₁-S₀ origin shifts for features labelled Aw₁

are $+6\text{ cm}^{-1}$ for FEB, -9 cm^{-1} for CEB and -11 cm^{-1} for BrEB, assuming that the BrEB cluster also has an *anti* host conformation.

Very low signals prevented the recording of any IR-UV ion depletion spectra for FEB.w₁ clusters. For BrEB.w₁ only the OH stretch region was measurable while for CEB.w₁ both CH and OH stretch regions were able to be recorded. The CH stretch region probing the CEB.w₁ origin shown in figure 5c is somewhat congested, suggesting the possibility of contributions from more than one cluster. However, the most intense spectral features are similar to the *anti* host conformer, most notably a single, broad band in the aromatic region at 3043 cm^{-1} . The 2888 cm^{-1} band corresponds to the *anti* spectrum, and the lack of the *gauche* 2925 cm^{-1} band suggests there is minimal contribution from any cluster with *gauche* host conformation. In the OH stretch region (figure 8a) of CEB.w₁, two strong bands at 3621 cm^{-1} and 3737 cm^{-1} were observed and assigned to the symmetric (ν_1) and antisymmetric (ν_3) stretches of water. The BrEB.w₁ spectrum in figure 8b shows two similarly strong bands at 3618 cm^{-1} and 3738 cm^{-1} . For comparison, these modes are found at 3657 cm^{-1} and 3756 cm^{-1} in the free water molecule. The modest red shifts seen in the clusters and ν_1/ν_3 separation of 116 cm^{-1} and 120 cm^{-1} for CEB.w₁ and BrEB.w₁ respectively, suggest the presence of a weakly donating water molecule. Either the halogen atom or the pi system of the aromatic ring could serve as the H-bond acceptor site. However, the small magnitude ($<10\text{ cm}^{-1}$) of the solvent induced S₁-S₀ origin shifts argues against assignment to pi-bound clusters. OH...pi interaction of a water molecule leads to significant blue-shifts of $+49\text{ cm}^{-1}$ in benzene³² and $+52\text{ cm}^{-1}$ in 2-phenylethanol.³³ Additionally, the presence of intact parent ion suggests the clusters are not pi-bound. Ionisation of ethylbenzene derivatives typically occurs at the phenyl ring, causing fragmentation of the cluster upon ionisation, due to the repulsive geometry in the cationic cluster.³²

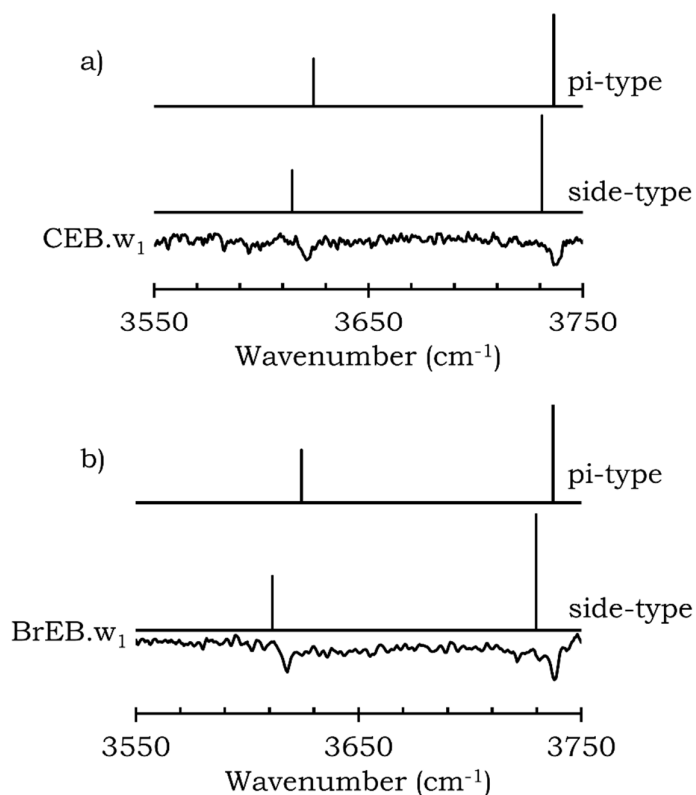


Figure 8. OH stretch spectra for a) CEB.w₁ and b) BrEB.w₁ and MP2/def2-TZVPP harmonic frequency stick spectra (scaling factor derived empirically from Figure 9.)

Trace amounts of signal in the FEB.w₁ mass channel at 37676 cm⁻¹ are tentatively assigned to a side-water cluster of the *gauche* host conformer. No other *gauche* clusters were experimentally observable, which warrants some comment. At B3LYP-D3(BJ)/aug-cc-pVTZ level, binding energies for *gauche*-side clusters are comparable to the anti clusters, but *gauche*-pi structures are more stable than their *anti*-counterparts by up to 5 kJ mol⁻¹. If, as expected, *gauche*-pi (or indeed *anti*-pi) structures are populated in the jet, ionisation-induced dissociation would empty the XEB.W₁⁺ mass channel and produce only XEB⁺ daughter ions whose

signal could be swamped by the much more abundant monomer-derived signal. It is also possible that the energy associated with binding a water molecule may be harnessed to overcome the barrier for rotation of the alkyl side-chain, allowing interconversion from *gauche* to *anti*.

Discussion

Monomers

Ethylbenzene derivatives can be divided into two broad classes; those which have significant stabilising effects between the substituent and the phenyl ring (such as those with H-bond donating substituents such as amines or alcohols), and those which have either minimal or repulsive effects. Halogens fall into the latter category. A repulsive interaction between the π -electrons of the phenyl ring and the electronegative halogen atom results in the *anti* conformer being energetically preferred. The extent of this repulsion would appear to be correlated with the size and polarisability of the halogen atom.

Relative energy differences between *anti* and *gauche* conformers of BrEB adhered to trends previously observed in FEB and CEB by Martin *et al.* Similar electronic origin heights would imply the *anti* conformer is preferred by approximately 2-3 kJ mol⁻¹, due to the double degeneracy of the *gauche* conformer. This experimental trend is supported at all levels of theory, with the exception of MP2/aug-cc-pVTZ.

FEB origin bands A and G are split by 50 cm⁻¹ while the CEB origin bands overlap. This splitting between origin bands has been attributed previously to interaction between the functional group at the terminus of the ethyl sidechain and the conjugated π -system of the aromatic ring.³⁴ However, the notion that a *gauche* conformer must have a red-shifted origin has been previously dispelled, for

example, benzenepropanitrile (BPN) has a *gauche* origin +16 cm⁻¹ to the blue of its *anti* counterpart,²⁵ as does 3-phenyl-1-propanoic acid (Δ +22 cm⁻¹).³⁴ BrEB similarly fails to adhere to this heuristic, with the 0-0 transition of the *gauche* conformer found +17 cm⁻¹ to the blue of the *anti*.

Clusters and H-bonding

In all three *anti* XEB species, hydrogen bonding to the halogen is in direct competition with donation to the π -electrons of the aromatic ring. This gives a useful benchmark against which to measure the strength of each halogen as a hydrogen bond acceptor. In all instances, clusters with OH...X interactions were energetically favourable by 2-3 kJ mol⁻¹ from coupled-cluster calculations, compared to their π -donating counterpart. This relative trend is observed at all levels of theory and for all XEB species, with the notable exception of MP2/def2-TZVPP, and only once zero-point energies are accounted for. Confidence in a side-type assignment for CEB.w₁ and BrEB.w₁ is encouraged by several factors; intact parent ion signal argues against pi-bound water clusters, the spectral shift of the electronic origin is small and a strong correlation is found between computed and experimentally assigned vibrational OH bands (ν_1) of water donating to various organic functional groups seen in Figure 9.

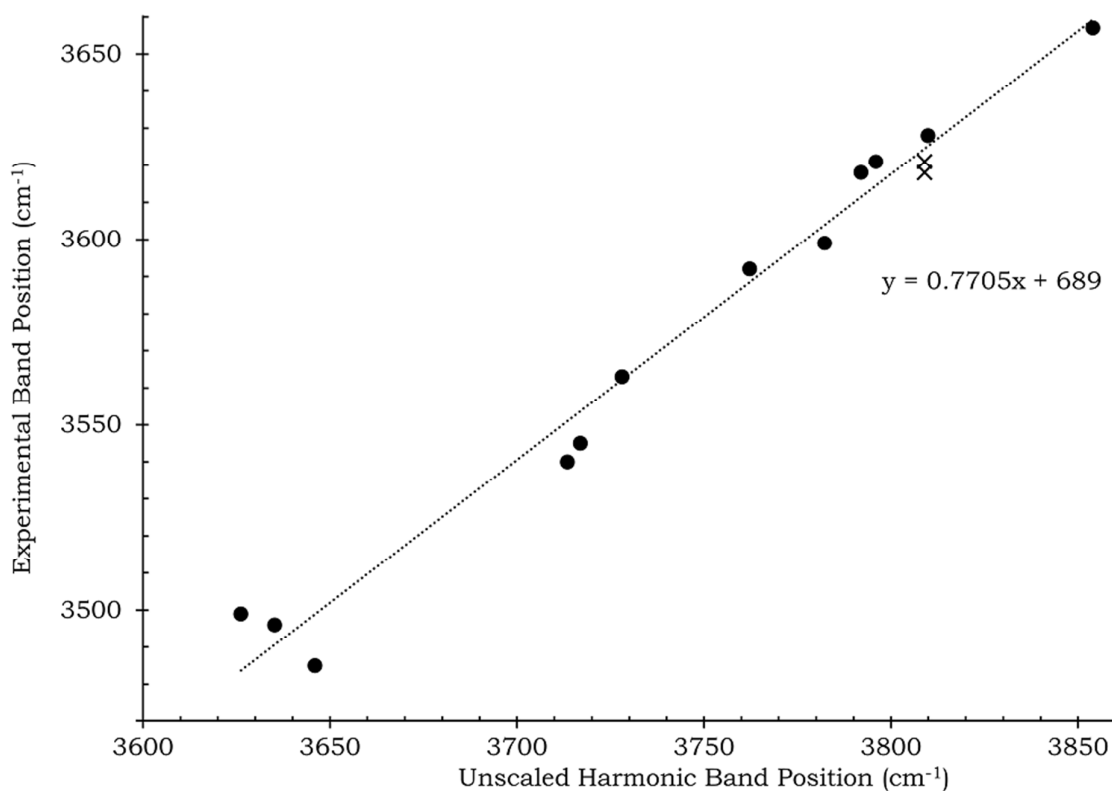


Figure 9. Experimental ν_1 OH band positions (cm^{-1}) for water donating to various functional groups (see table S2) plotted against unscaled harmonic band positions (cm^{-1}) calculated at MP2/def2-TZVPP level. X labels denote alternative assignment to CEB and BrEB anti π -type structures.

The magnitude of the red-shift is modest in the symmetric OH stretch of water that is hydrogen-bond donating to halogens, suggesting the overall acceptor strength of halocarbons is weak. The ν_1 red-shift of 36 cm^{-1} for CEB.w₁ and 39 cm^{-1} for BrEB.w₁ places these larger, diffuse halogens as stronger H-bond acceptors than nitrile π -electrons ($\Delta \nu_1 = 29 \text{ cm}^{-1}$)¹⁴, or benzene ($\Delta \nu_1 = 23 \text{ cm}^{-1}$)³⁵ but weaker than those of a nitrile lone pair ($\Delta \nu_1 = 56 \text{ cm}^{-1}$)¹⁴, and significantly weaker than other organic functional groups (NH₂, OH, C=O). The shift in the corresponding FEB cluster, although not experimentally measured, is expected to be smaller than for CEB by *ca.* 9 cm^{-1} based on MP2/def2-TZVPP results.

Turning the focus to molecular geometry, previous work within the group has noted the crucial role of secondary interactions (e.g. C-H...O) in stabilising weakly bound clusters.¹⁴ It is clear from predicted geometries of XEB side-type clusters that the larger halogen atoms (Br and Cl) facilitate potential secondary interactions with hydrogen atoms on the alpha or beta carbons more effectively than the less polarisable fluorine atom. This angular lability can be attributed to the well-established anisotropic charge distribution along the X-M covalent bond within metal-halides or the X-C bond in halocarbons.^{9,27,36} The net result is a region of negative electrostatic potential (ESP) located perpendicular to the X-C bond axis, and a region of positive ESP on the tip of the halogen atom (σ -hole). As the size of the halogen increases, the effect becomes more pronounced and thus incoming H-bond donor angles become more shallow, which facilitates secondary stabilising interactions. Fluorocarbons do not form σ -holes, in part, because highly electronegative fluorine atoms are unable to redistribute their electron density.^{37,38}

In any discussion of organic halides as hydrogen bond acceptors, it is prudent to note that fluorine defies most common trends. At first thought, fluorine would appear to be a strong candidate as a hydrogen bond acceptor (being the most electronegative element on the periodic table), yet literature precedents are few and far between.¹⁰ There is no doubt that the fluoride ion (F⁻) acts as a very strong proton acceptor, and metal-fluorides have been shown to be strong hydrogen bond acceptor species.³⁹ However, this trend fails to hold for covalently bound organic fluorine.³⁷ The importance of electronegativity in hydrogen bonding has been discussed since the genesis of the term “hydrogen bond”, with Pauling’s statement that “only the most electronegative atoms should form hydrogen bonds, and the strength of the bond should increase with the increase in electronegativity...”.⁴⁰ The importance of electronegativity in hydrogen bond donor species (D-H) should not be understated. The greater the electronegativity of D, the greater the effective positive

charge on the hydrogen atom. However, the relevance to hydrogen bond acceptors is less clear, being a measure of electron affinity rather than proton affinity. On the one hand, the best hydrogen bond acceptor atoms are highly electronegative (oxygen, nitrogen), but on the other, fluorocarbons appear to be very weak hydrogen bond acceptors. The underlying cause for this may be rooted in the importance of charge transfer in the formation of a hydrogen bond.³⁹ Larger, more diffuse halogen atoms allow for greater charge transfer from the acceptor atom to the donor atom, whereas charge transfer from the more tightly held electron density of fluorine is negligible, due to the low energy of the lone pair orbitals.

Conclusions

Monomers and singly-hydrated clusters of 2-fluoroethylbenzene (FEB), 2-chloroethylbenzene (CEB) and 2-bromoethylbenzene (BrEB) have been studied using a combination of resonant two-photon ionisation spectroscopy, infrared ion depletion spectroscopy and *ab initio* quantum chemical calculations. For each halogen species, two stable conformers were identified in the jet and assigned to *anti* and *gauche* conformers. 1:1 Hydrate clusters were also identified for each halogen species in the *anti* host conformer. Infrared spectra in the CH stretch region show a characteristic splitting of aromatic modes in the *gauche* conformer of FEB, CEB and BrEB species. The highest wavenumber CH stretch mode, the antisymmetric C₆H₂ stretch, blue-shifts as the size of the halogen substituent increases.

Two potential structures for these water clusters were proposed: insertion of water to the side of the X-C bond, or the less favourable coordination to the phenyl ring. Infrared spectra of chloro and bromo species were recorded in the OH stretch region, and CH stretch spectra recorded for the chloro species. CH stretch spectra

confirmed the host species as the *anti* conformer, and harmonic frequency calculations and the presence of intact parent ions, support a side-type water cluster. The strength of organic halides as hydrogen bond acceptors is generally weak for all halogen species, although the larger, more polarisable halogens show less angular specificity, which allows for secondary interactions to stabilise the greater structure.

Acknowledgements

The investigators would like to acknowledge the Australian Research Council (ARC) for funding support via project grant DP120100100 and linkage equipment grant LE100100131. La Trobe University provided a scholarship for Patrick Robertson. Quantum chemical calculations were carried out using facilities at Australia's National Computational Infrastructure National Facility (NCI-NF) under NCMAS grant ia1. The authors are indebted to Dr E. Sibert for helpful advice on the simplified anharmonic model and for generously supplying associated Fortran codes.

References

- 1 H. M. Lee, D. Kim and K. S. Kim, Structures, spectra, and electronic properties of halide-water pentamers and hexamers, $X^-(H_2O)_{5,6}$ ($X=F, Cl, Br, I$): Ab initio study, *J. Chem. Phys.*, 2002, **116**, 5509.
- 2 B. S. Ault, Infrared spectra of argon matrix-isolated alkali halide salt/water complexes, *J. Am. Chem. Soc.*, 1978, **100**, 2426–2433.
- 3 C. Turrd, C. K. Chang, G. E. Leroi, R. I. Cukier and D. G. Nocera, Photoinduced Electron Transfer Mediated by a Hydrogen-Bonded Interface, *J.*

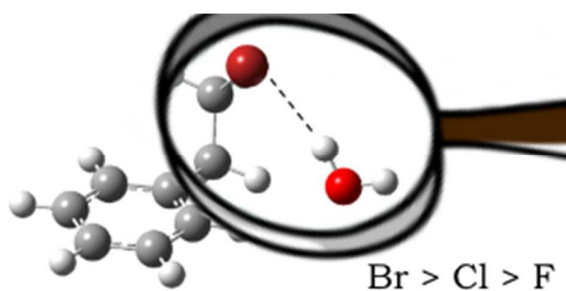
- Am. Chem. Soc.*, 1992, **2**, 4013–4015.
- 4 W. H. Robertson, E. A. Price, J. M. Weber, J. Shin, G. H. Weddle, M. A. Johnson, Y. U. V, P. O. Box and N. H. V, Infrared Signatures of a Water Molecule Attached to Triatomic Domains of Molecular Anions : Evolution of the H-bonding Configuration with Domain Length, 2003, **0**, 6527–6532.
- 5 J. E. Grebel, J. J. Pignatello and W. A. Mitch, Effect of halide ions and carbonates on organic contaminant degradation by hydroxyl radical-based advanced oxidation processes in saline waters, *Environ. Sci. Technol.*, 2010, **44**, 6822–6828.
- 6 R. Mancinelli, A. Botti, F. Bruni, M. A. Ricci and A. K. Soper, Hydration of sodium, potassium, and chloride ions in solution and the concept of structure maker/breaker, *J. Phys. Chem. B*, 2007, **111**, 13570–13577.
- 7 R. S. MacTaylor and A. W. Castleman Jr., Cluster Ion Reactions: Insights into Processes of Atmospheric Significance, *J. Atmos. Chem.*, 2000, **36**, 23–63.
- 8 V. Grignard, Mixed organomagnesium combinations and their application in acid, alcohol, and hydrocarbon synthesis, *Ann. Chim*, 1901, **24**, 433–490.
- 9 P. Metrangolo, H. Neukirch, T. Pilati and G. Resnati, Halogen bonding based recognition processes: A world parallel to hydrogen bonding, *Acc. Chem. Res.*, 2005, **38**, 386–395.
- 10 L. Brammer, E. A. Bruton and P. Sherwood, Understanding the Behavior of Halogens as Hydrogen Bond Acceptors, *Cryst. Growth Des.*, 2001, **1**, 277–290.
- 11 E. J. Bieske, Spectroscopic studies of anion complexes and clusters: A microscopic approach to understanding anion solvation, *Chem. Soc. Rev.*, 2003, **32**, 231.

- 12 P. Ayotte, J. A. Kelley, S. B. Nielsen and M. A. Johnson, Vibrational spectroscopy of the F-H₂O complex via argon predissociation : photoinduced , intracuster proton transfer ?, 2000, 455–459.
- 13 D. E. Martin, E. G. Robertson, R. J. S. Morrison and B. Dobney, Resonant two-photon ionization and ab initio conformational analysis of haloethyl benzenes (PhCH(2)CH(2)X,X=Cl,F)., *J. Chem. Phys.*, 2007, **127**, 134307.
- 14 P. A. Robertson, I. A. Lobo, D. J. D. Wilson and E. G. Robertson, Nitriles as directionally tolerant hydrogen bond acceptors: IR-UV ion depletion spectroscopy of benzenepropanenitrile and its hydrate clusters, , DOI:10.1016/j.cplett.2016.08.029.
- 15 I. a Lobo, D. J. D. Wilson, E. Bieske and E. G. Robertson, A sting in the tail of flexible molecules: spectroscopic and energetic challenges in the case of p-aminophenethylamine., *Phys. Chem. Chem. Phys.*, 2012, **14**, 9219–29.
- 16 G. S. Lal, G. P. Pez, R. J. Pesaresi, F. M. Prozonic and H. Cheng, Bis (2-methoxyethyl) aminosulfur Trifluoride : A New Broad-Spectrum Deoxofluorinating Agent with Enhanced Thermal Stability Bis (2-methoxyethyl) aminosulfur Trifluoride : A New, *J. Org. Chem.*, 1999, 215–216.
- 17 D. J. Frisch, M. J.; Trucks, G. W.; Schlegel, H. B.; Scuseria, G. E.; Robb, M. A.; Cheeseman, J. R.; Scalmani, G.; Barone, V.; Mennucci, B.; Petersson, G. A.; Nakatsuji, H.; Caricato, M.; Li, X.; Hratchian, H. P.; Izmaylov, A. F.; Bloino, J.; Zheng, G.; Sonnenb, *Gaussian, Inc., Wallingford CT*, 2013.
- 18 S. Grimme, Density functional theory with London dispersion corrections, *Wiley Interdiscip. Rev. Comput. Mol. Sci.*, 2011, **1**, 211–228.
- 19 E. L. Sibert, N. M. Kidwell and T. S. Zwier, A first-principles model of fermi

- resonance in the alkyl CH stretch region: Application to hydronaphthalenes, indanes, and cyclohexane, *J. Phys. Chem. B*, 2014, **118**, 8236–8245.
- 20 E. G. Buchanan, E. L. Sibert and T. S. Zwier, Ground state conformational preferences and CH stretch-bend coupling in a model alkoxy chain: 1,2-diphenoxyethane, *J. Phys. Chem. A*, 2013, **117**, 2800–2811.
- 21 E. L. Sibert, Dressed local mode Hamiltonians for CH stretch vibrations, *Mol. Phys.*, 2013, **111**, 2093–2099.
- 22 D. P. Tabor, D. M. Hewett, S. Bocklitz, J. A. Korn, A. J. Tomaine, A. K. Ghosh, T. S. Zwier and E. L. Sibert, Anharmonic modeling of the conformation-specific IR spectra of ethyl, n -propyl, and n -butylbenzene, *J. Chem. Phys.*, 2016, **144**, 0–11.
- 23 R. T. Kroemer, K. R. Liedl, J. A. Dickinson, E. G. Robertson and J. P. Simons, Conformationally induced changes in the electronic structures of some flexible benzenes. A molecular orbital model, *J. Am. Chem. Soc.*, 1998, **120**, 12573–12582.
- 24 D. W. Pratt, High resolution spectroscopy in the gas phase: even large molecules have well-defined shapes., *Annu. Rev. Phys. Chem.*, 1998, **49**, 481–530.
- 25 D. E. Martin, E. G. Robertson and R. J. S. Morrison, A conformational study of gaseous benzenepropanenitrile by resonant 2-photon ionisation spectroscopy, *Chem. Phys. Lett.*, 2006, **425**, 210–215.
- 26 A. Courty, M. Mons, I. Dimicoli, F. Piuze, M. P. Gageot, V. Brenner, P. de Pujo and P. Millié, Quantum effects in the threshold photoionization and energetics of the benzene-H₂O and benzene-D₂O complexes: Experiment and simulation, *J. Phys. Chem. A*, 1998, **102**, 6590–6600.

- 27 M. Kolář, J. Hostaš and P. Hobza, The strength and directionality of a halogen bond are co-determined by the magnitude and size of the σ -hole, *Phys. Chem. Chem. Phys.*, 2014, **16**, 9987–9996.
- 28 I. A. Lobo, The Chemical Shape of Life : Laser Spectroscopy Studies of Gas Phase Conformation in Biomolecules and their Clusters, *PhD Thesis, La Trobe Univ.*
- 29 G. Varsányi, *Vibrational spectra of benzene derivatives*, Elsevier, 2012.
- 30 T. Shimanouchi, Tables of Molecular Vibrational Frequencies Consolidated Volume 1., <http://webbook.nist.gov/cgi/cbook.cgi?Source=1972SHI1-160B&Units=SI&Mask=800>.
- 31 P. Hobza and Z. Havlas, Blue-Shifting Hydrogen Bonds, *Chem. Rev.*, 2000, **100**, 4253–4264.
- 32 R. N. Pribble and T. S. Zwier, Size-Specific Infrared Spectra of Benzene-(H₂O)_n Clusters (n = 1 through 7): Evidence for Noncyclic (H₂O)_n Structures., *Science*, 1994, **265**, 75–79.
- 33 M. Mons, E. G. Robertson, L. C. Snoek and J. P. Simons, Conformations of 2-phenylethanol and its singly hydrated complexes: UV–UV and IR–UV ion-dip spectroscopy, *Chem. Phys. Lett.*, 1999, **310**, 423–432.
- 34 E. G. Robertson, J. P. Simons and M. Mons, Comment on ‘Structural and Vibrational Assignment of p-Methoxyphenethylamine Conformers’, *J. Phys. Chem. A*, 2001, **105**, 9990–9992.
- 35 T. S. Zwier, The Spectroscopy of Solvation in Hydrogen Bonded Aromatic Clusters, *Annu. Rev. Phys. Chem.*, 1996, **47**, 205–241.
- 36 T. Clark, M. Hennemann, T. Clark, M. Hennemann, J. S. Murray and P.

- Politzer, Halogen bonding : the σ -hole, , DOI:10.1007/s00894-006-0130-2.
- 37 J. D. Dunitz and R. Taylor, Organic Fluorine Hardly Ever Accepts Hydrogen Bonds, *Chem. - A Eur. J.*, 1997, **3**, 89–98.
- 38 L. Brammer, E. A. Bruton and P. Sherwood, Fluoride ligands exhibit marked departures from the hydrogen bond acceptor behavior of their heavier halogen congeners, *New J. Chem.*, 1999, **23**, 965–968.
- 39 W. H. Thompson and J. T. Hynes, Frequency shifts in the hydrogen-bonded OH stretch in halide - water clusters. The importance of charge transfer, *J. Am. Chem. Soc.*, 2000, **122**, 6278–6286.
- 40 L. Pauling, *The nature of the chemical bond and the structure of molecules and crystals: an introduction to modern structural chemistry*, Cornell university press, 1960, vol. 18.

Table of Contents Entry

The hydrogen bond acceptor strength of a series of halocarbons is studied by electronic and vibrational spectroscopy